Ultrasonics Sonochemistry 18 (2011) 795–800

Contents lists available at ScienceDirect

Ultrasonics Sonochemistry

journal homepage: www.elsevier.com/locate/ultsonch

Effect of ultrasonic irradiation on crystallization kinetics of potassium dihydrogen phosphate

Perviz Sayan *, Sibel Titiz Sargut, Bercem Kiran

Marmara University, Faculty of Engineering, Chemical Engineering Department, Goztepe Campus, TR-34722 Istanbul, Turkey

ARTICLE INFO

Article history:
Received 29 July 2010
Received in revised form 2 November 2010
Accepted 3 November 2010
Available online 13 November 2010

Keywords:
Ultrasound power
Potassium dihydrogen phosphate
MSMPR crystallizer
Size-dependent growth
ASL model

ABSTRACT

The ultrasound effect applied on potassium dihydrogen phosphate was investigated in a continuous crystallization system. The studied process variables were ultrasonic power (W) and residence time. The crystal size distributions of the final products obtained with and without ultrasonic power were determined and the data were evaluated by using modified form of Abegg, Stevens and Larson (ASL) model. The supersaturation limit decreased with ultrasonic waves and the crystal morphology was modified. The average crystal size decreased in the presence of ultrasonic power. An abrasive effect was observed at a high ultrasonic power input.

1. Introduction

The present trend from users to apply ultrasound to initiate and control crystallization processes. In the near future as ultrasound allows a new dimension of control over the nucleation regime, and may allow the nucleation-crystal growth balance to be regulated in order to optimize the product and particle properties [1]. Ultrasound can enhance the rates of mass transfer and reaction in heterogeneous systems, since ultrasound causes a decrease in the diffusion layer thickness on the solid–liquid interfaces in the suspension [2–6]. Many of the effects produced by ultrasonic in solid–liquid and liquid systems are associated with the production of cavitation. The cavitation from ultrasonic itself has both physical and chemical effects [7]. Ultrasound is known to influence the crystallization system in several ways such as reduction in induction time for crystallization, reduction in amount of antisolvent required for crystallization, narrowing down crystal size distribution with simultaneous reduction in dominant crystal size and change in crystal geometry [8]. Amara et al. have proved that the average crystal size of potash alum crystals decreases with an increase of ultrasonic power and ultrasonic waves modify the morphology of potash alum crystals produced [9]. Chow et al. studied the effect of high intensity ultrasonics in sucrose solutions [10]. They reported that primary and secondary nucleation of ice can be modified by high intensity ultrasonics. In another study, the mechanism of the ultrasonic effect on homogeneous nucleation of barium sulfate has been analyzed and it has been reported that the main effect of ultrasound is to increase the diffusion coefficient [11]. Moholkar et al. showed that nucleation rate of potassium chloride increased with intensity of ultrasound while growth rate (and hence the dominant crystal size) reduced as compared to the mechanically agitated system [12]. Lyczko et al. showed that ultrasound irradiation narrows down the metastable zone width by simultaneously enhancing the rate of nucleation [13].

A continuously operated mixed-suspension mixed-product removal crystallizer (MSMPR) is a recommended device to determine the main kinetic parameters, crystal growth rate and effective rate of nucleation, which influence crystal size distribution (CSD) [14]. In this study the effect of ultrasonic irradiation on crystallization kinetics of potassium dihydrogen phosphate which is an important substance in industrial processes is presented. For this study it is aimed to clarify the effect of ultrasound on the population density, average particle size and the crystal habit using size dependent growth (modified ASL Model) [15,16].

2. Theory

Crystallization process consists of three basic steps which are achievement of supersaturation, formation of nuclei and growth of crystals. The rate of nucleation (B^o) is the number of new particles formed per unit time per unit volume of solution. It is affected from supersaturation level Δc, suspension density (M_T) and the fluid dynamics. These effects can be expressed with the power-law relation at constant power input and geometry:

* Corresponding author. Tel.: +90 216 348 02 92; fax: +90 216 348 02 93.
E-mail address: perviz.sayan@marmara.edu.tr (P. Sayan).

1350-4177/$ - see front matter © 2010 Elsevier B.V. All rights reserved.
doi:10.1016/j.ultsonch.2010.11.003

Nomenclature

a, b	ASL model parameters (−)
B^o	nucleation rate ($m^{-3}\ s^{-1}$)
Δc	supersaturation (kg salt m^{-3} solution)
g	order of growth rate (−)
G	overall linear growth rate ($m^3\ s^{-1}$)
G^o	growth rate of nuclei (ASL model) ($m\ s^{-1}$)
i	kinetic order (−)
j	order of suspension density (−)
k_2, k_n	nucleation rate constant (−)
k_G	overall growth rate constant (−)
L	crystal size (m)
M_T	suspension density ($kg\ m^{-3}$)
n	population density (number $m^{-1}\ m^{-3}$)
n^o	population density of nuclei (number $m^{-1}\ m^{-3}$)
p	number of experimental points (−)
Q	withdrawal rate of crystallizer content ($m^3\ s^{-1}$)
t	time (s)
V	volume of crystallizer (m^3)

Greek letters

α	volume shape factor (−)
ρ	crystal density ($kg\ m^{-3}$)
τ	residence time (s)

$$B^o = k_2 \Delta c^i M_T^j \tag{1}$$

After formation of stable nuclei, they begin to grow into visible crystals. Two steps in mass deposition process are suggested. These are the diffusion from bulk of the solution to crystal surface and the reaction on the crystal surface. The overall growth rate (G) is the rate of change of the crystal size (L) with time and is expressed as

$$G = \frac{dL}{dt} = k_G \Delta c^g \tag{2}$$

In general, nucleation rate is expressed in terms of the growth rate since it is difficult to measure supersaturation:

$$B^o = k_n G^i M_T^j \tag{3}$$

The number of crystals corresponding to a particulate size, L, is termed as population density (n). The population density can be expressed as

$$\frac{d(nG)}{dL} + \frac{n}{\tau} \tag{4}$$

where τ is the residence time. Eq. (4) refers to a well mixed steady state crystallizer with clear liquor feed, where the particle size only changes owing to crystal growth. Here, both agglomeration and attrition are neglected and the crystal size distribution (CSD) and magma density of particles in the product outflow are the same as in the crystallizer mixed product removal. If the growth rate is size independent, i.e. Mc Cabe's ΔL law is valid,

$$n = n^o \exp\left(-\frac{L}{G\tau}\right) \tag{5}$$

the crystal growth rate may be determined from the slope of semi-logarithmic population density graph while the intercept of the line gives the value of $\ln(n^o)$. Nucleation rate can be determined as

$$B^o = n^o G \tag{6}$$

and the kinetic orders i and j can be determined from Eq. (3). Kinetic parameter, i, is defined as the coefficient of sensitivity of nucleation with respect to crystal growth.

If the growth rate is size dependent, a more complex model of a process kinetics giving consideration to a strong curvature of a $\ln n(L)$ dependency observed in the initial L range and, thus, a considerably higher n_o values, requires establishing of some $G(L)$ dependency form and then, after introducing into, solving an equation:

$$-\int_{n_o}^{n} \frac{dn}{n(L)} = \int_0^L \frac{dL}{G(L)\tau} + \int_{G_o}^{G} \frac{dG(L)}{G(L)} \tag{7}$$

Abegg, Stevens and Larson (ASL) proposed a solution of Eq. (7) as analytical expression $n(L)$ comply with assumed $G(L)$ form as the following:

$$G(L) = G^o(1 + aL)^b \tag{8}$$

This empirical equation is capable of describing systems where growth rate is inversely proportional to the size of particles. On the other hand, there is a difficulty in finding out the nuclei density when the population balance of ASL equation is used [17]. Jancic and Garside had shown that extrapolation of experimental points may lead to very different results in nuclei size [18]. Results may change depending on the extrapolation method and measuring technique of particle size distribution. In this study, only standard ASTM sieve series were used to measure the particle size distribution, and modified form of the extrapolation methods suggested by Jancic was used [16]. In the proposed model the smallest particle size which we could measure with the laboratory sieve was selected and standardization procedure was applied. In all experiments the smallest particle size is taken as an average value of 90 μm and 106 μm sieve. Under this condition the growth rate which is dependent on particle size can be written as follows:

$$G = G^*[1 + a(L - L^*)]^b \tag{9}$$

where G^* is the growth rate for particles in 98 μm average size. Substituting the growth rate G (Eq. (9)) in Eq. (4) and integrating Eq. (4), the following population density equation is obtained:

$$n(L) = n^*[1 + a(L - 98)]^{-b} \exp\left[\frac{1 - (1 + a(L - 98))^{1-b}}{1 - b}\right] \tag{10}$$

where $a = \frac{1}{G^*\tau}$. The growth rate of nuclei G^*, nuclei number density n^*, and exponent of size dependency b are obtained by fitting the experimental data to the above equation (Eq. (10)). The parameter b is usually less than 1. When $b = 0$ model is turn to model of independent particle size. The growth rate increases with size volume and vice versa when b is positive. In this case nucleation rate can be expressed:

$$B^* = n^* \cdot G^* \tag{11}$$

where n^* is the nuclei density for particles in 98 μm average size.

3. Experimental

In this study the laboratory scale MSMPR crystallizer shown in Fig. 1 was used.

Potassium dihydrogen phosphate (KDP) used in this study was analytical grade and was purchased from Merck Company. Experiments were performed in a 0.5 L jacketed glass crystallizer with a

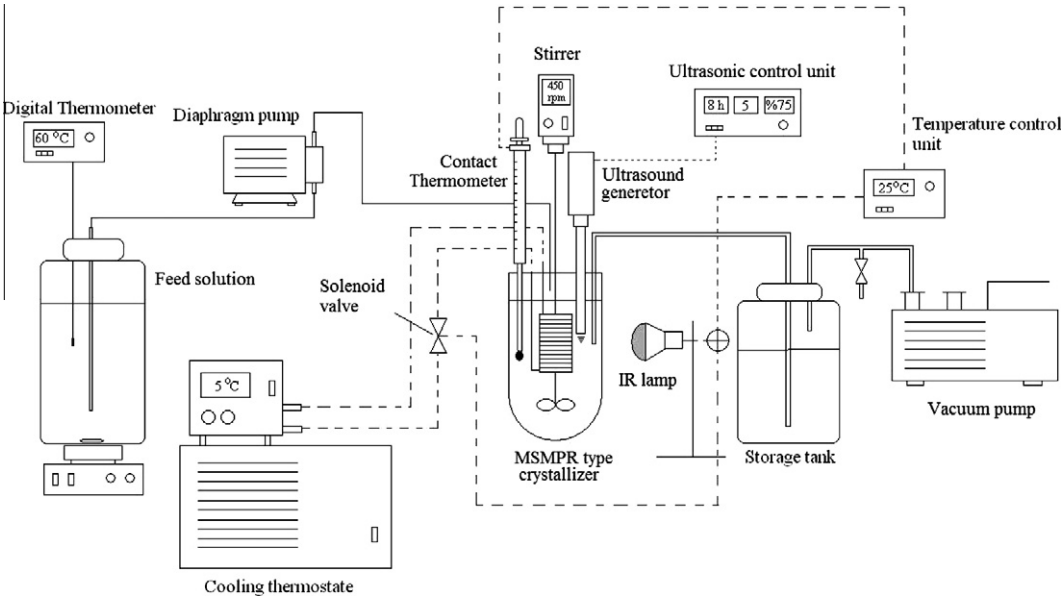

Fig. 1. Experimental set-up.

U-shaped bottom, which was equipped with a three blade impeller and three baffles. The impeller was rotated at a speed of 250 rpm to ensure all the particles were well suspended. Saturated solution of KDP at 35 °C was prepared on the basis of the solubility data published by Mullin [15]. Solution was heated to 40 °C, 5 °C above the saturation temperature, to ensure complete dissolution of the solute and then fed into the crystallizer. Supersaturation was achieved by cooling the solution to 20 °C lower temperature than the saturation temperature of the solution. Precise temperature control in the crystallizer was achieved by thermostat system. KDP solution was fed into the crystallizer by peristaltic pump. Experiments were conducted at three different residence times and four different ultrasonic powers. Bandelin Sonoplus HD 2200 ultrasonic power supplier was used to produce different ultrasonic powers. A piezoelectric ultrasonic transducer transforms a sinusoidal electrical voltage into mechanical longitudinal resonance vibration, where the resonance frequency of the equipment is 20 kHz and the equipment had 200 W HF-output. Ultrasonic energy was introduced into the system via an ultrasonic horn (titanium alloy Ti-6Al-4 V). The ultrasonic probe used had a cylindrical shape with a diameter of 3 mm (surface area 0.071 cm^2). Output settings were adjusted within a range of 8–60 W. The system was run for a period of eight residence times in order to attain a steady state in the crystallizer. Then the characteristic suspension sample was withdrawn at isokinetic velocity and crystals were separated from mother liquor by vacuum filtration. Crystals were dried in air before using for further studies. CSD was determined by sieving analyses using an ASTM E-11 sieve series in the range of 90–1000 μm. Sieve analyses results were evaluated by using the linearized form of population balance equation to determine the kinetic parameters [15]. The volume shape factor was determined by the method proposed by Harris using a second upper sieve in the sieve series for each fraction [19].

4. Results and discussion

A population balance was used to describe the nucleation and growth of crystals formed in the reactor. This population balance simplifies to form the MSMPR model. Fig. 2 shows the population density values versus crystal size for KDP crystals obtained from pure KDP solution at different residence times.

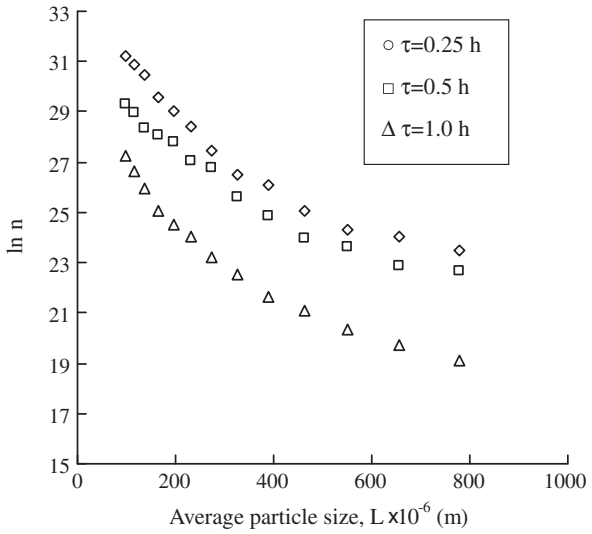

Fig. 2. Population density graph of KDP grown without ultrasonic power.

As it can be clearly seen from Fig. 2, the population density results indicate a deviation from linearity, and the population density distributions are concave to top. Similar behavior in population density was determined for all of the applied ultrasonic power degrees. This type of population density distribution can result from the occurrences of growth rate dispersion, secondary nucleation and size dependent difference in a relative fluid crystal velocity. However, it is impossible to distinguish between size-dependent growth on the one hand and growth dispersion on the other by analyses of MSMPR alone. In order to accommodate the concept of size-dependent growth, several empirical relationships between G and L have been proposed [20]. ASL (Abegg, Stevens and Larson) equation is the most widely used model. In this study the population density results were analyzed by considering ASL size-dependent growth model.

Eq. (10) was fitted to the population density data to obtain the model parameters G^*, n^*, and b. Table 1 gives the coefficients to be used to find size dependent growth rate of KDP with and without ultrasonic power according to the ASL model (Eq. (10)).

Table 1
ASL model parameters for KDP crystallization in the presence of ultrasonic power at different residence times.

Residence time, τ (s)	Ultrasonic power (W)	$G^* \times 10^{-8}$ (m s^{-1})	$a \times 10^4$ (m^{-1})	b	$n^* \times 10^{13}$ (m^{-1} m^{-3})	$B^* \times 10^5$ (m^{-3} s^{-1})
900	–	3.775	2.9433	0.59	3.724	14.06
1800	–	2.542	2.1855	0.51	0.534	1.36
3600	–	0.827	3.3589	0.54	0.0694	0.06
900	8	2.411	4.6085	0.45	5.007	12.07
	20	2.225	4.9938	0.46	6.013	13.38
	40	2.324	4.7810	0.45	3.621	8.42
	60	2.406	4.6181	0.41	6.579	15.83
1800	8	1.041	5.3367	0.54	2.476	2.58
	20	1.288	4.3133	0.45	4.120	5.31
	40	1.307	4.2506	0.45	4.006	5.24
	60	1.516	3.6646	0.54	2.598	3.94
3600	8	0.681	4.0790	0.51	3.860	2.63
	20	0.664	4.1834	0.38	1.061	7.05
	40	0.874	3.1782	0.53	2.653	2.32
	60	0.634	4.3814	048	7.425	4.71

Table 2
Relative deviation values of ASL model for KDP crystallization in the presence of ultrasonic power at different residence times.

Residence time (s)	Mean relative deviation (%) Ultrasonic power (W)				
	–	8	20	40	60
900	1.010	1.812	4.785	3.115	2.923
1800	1.169	4.595	2.080	1.569	1.931
3600	1.434	2.254	5.588	2.507	3.699

As can be seen from Table 1, the obtained parameter b is positive, meaning growth rate increases with size volume. The nucleation rate was calculated based on Eq. (11) and the results were also given in Table 1. It is clearly seen that nucleation rate decreases with increasing residence time.

For each $n(L)$ function (model) and experimental data set, relative deviation was calculated. Table 2 gives the mean relative deviation values.

By considering the analysis, mean relative deviation values vary between 1.010 and 5.588. It can be concluded that the ASL model fitted the experimental data well. Deviation between the experimental and the theoretical data for large particle size cause to obtain high mean relative deviation values. Fig. 3 can be given as an example showing the fitted population density of KDP crystals grown without ultrasonic power at a residence time of 0.5 h.

As can be seen from Fig. 3, this model fits the data. All results show that KDP is the system which appear to exhibit size-dependent growth under operating conditions. In literature, both microscopic and MSMPR studies showed that the growth rate of KDP crystals was considerably dependent on the crystal size and the size-dependency of growth rate increased with supersaturation [21–23].

The sieve analysis results were used in order to see the effect of ultrasonic power on the CSD of KDP. Fig. 4 shows the average particle size of KDP which is determined as 50% retained of cumulative oversize versus the ultrasonic power for different residence times.

As it is clearly seen from Fig. 4, the average particle size decreases in the range of 0–8 W ultrasonic power and then remains almost constant with increasing ultrasonic power. An increase in the mean residence time did not affect this tendency.

The photographs of crystals grown with and without ultrasonic power are given in Fig. 5 for 212 μm crystal size.

As can be seen from Fig. 5, when the ultrasonic power is not applied, the clear KDP crystals with a similar form and having minimum surface defect were obtained. By increasing the ultrasonic power to 8 W, the crystal surface defect increases, and as a result of this, a twin-like form becomes dominant. This behavior in-

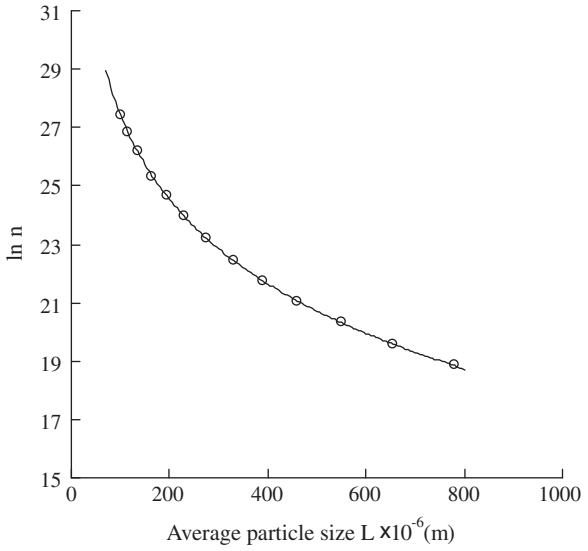

Fig. 3. Size dependent analysis of the population density data according to the ASL model. (UP = 0 W; τ = 3600 s).

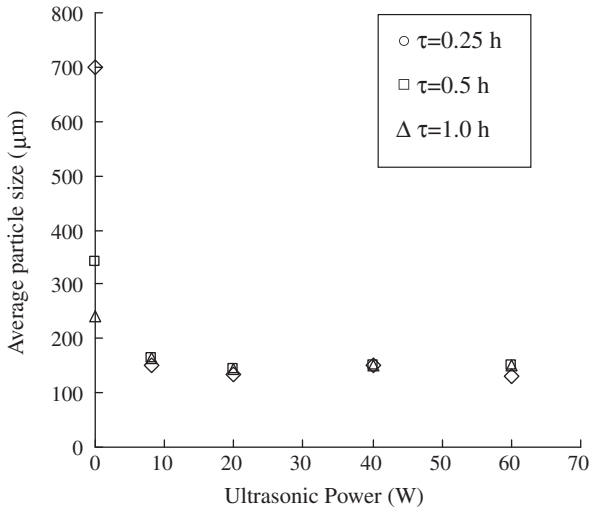

Fig. 4. Influence of ultrasonic power on the average particle size of KDP.

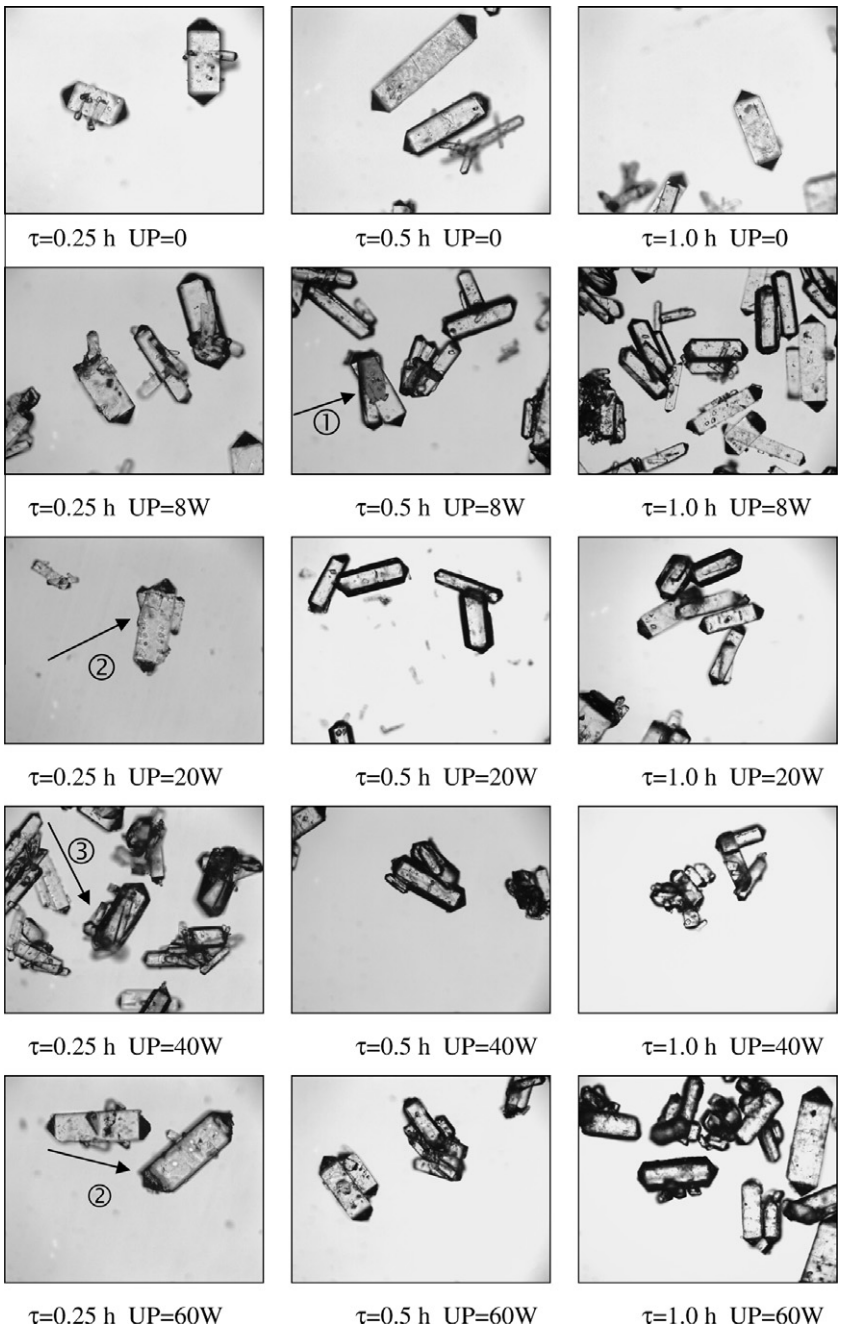

Fig. 5. KDP crystals (212 μm) obtained at different residence times and ultrasonic power (UP). (1) Twin formation, (2) cavitation effect and (3) defective growth.

creases with increasing residence time. At 20 W ultrasonic power, cavitation effects on the crystal surface are clearly observed. Furthermore, weak twin-like crystals seen at 8 W ultrasonic powers were broken and these detached fragments grow individually at 20 W ultrasonic power. At 40 W ultrasonic powers, crystal defects began to occur and this affected the sizes of the nuclei. This situation occurred on all crystal growth steps. As a result of this, undefined shaped crystals were obtained and this effect increased with increasing residence time. It was also observed that KDP crystals grew layer by layer at 40 W ultrasonic power. As can be seen from Fig. 5, the cavitation bubbles drastically damage the smooth edges of the KDP crystals at 60 W ultrasonic powers. Thus, the crystals lost their own shapes. Furthermore, this situation also enhances the secondary nucleation.

5. Conclusion

The effect of ultrasonic irradiation and crystallization kinetics of potassium dihydrogen phosphate at different residence times was presented. The calculation procedure for the ideal MSMPR crystallizer was applied assuming size dependent growth (modified ASL Model). It should be emphasized that the kinetic data present the growth of KDP crystals is size dependent with and without ultrasound action. On the basis of experimental data, using modified form of ASL Model, the following parameters: n^*, G^*, B^*, a, and b values were determined. b values were found as positive meaning growth rate increases with size-volume for all investigated conditions. The results show that the ultrasound action in crystallization medium affect nucleation rate and growth rate, and in turn the

crystal size distribution. The ultrasound waves are expected to increase the nucleation rate in the system. The modification in the crystal shape results from the presence of ultrasonic waves in the crystallization media. The ultrasound waves caused the occurrence of some defects on crystal surfaces and the shape of the crystals changed as twin-like form dominantly. The crystals obtained in the presence of ultrasound are smaller than those obtained without ultrasound for all residence times. The mean size of KDP crystals obtained without ultrasound decreases four times in the presence of 8 W ultrasonic power but an increase of power has no notable effect on crystal size. ASL model was found to be suitable to express the growth rate of KDP crystals grown in KDP solution with and without ultrasonic power.

References

[1] M.D. Luque de Castro, F. Priego-Capote, Ultrasound assisted crystallization (sonocrystallization), Ultrason. Sonochem. 14 (2007) 717–724.

[2] L.C. Hagenson, S.D. Naik, L.K. Doraiswamy, Rate enhancements in a solid–liquid reaction using PTC, microphase, ultrasound and combinations thereof, Chem. Eng. Sci. 49 (1994) 4787–4800.

[3] L.C. Hagenson, L.K. Doraiswamy, Comparison of the effects of ultrasound and mechanical agitation on a reacting solid–liquid system, Chem. Eng. Sci. 53 (1998) 131–148.

[4] N. Lyczko, M. Hassoun, F. Espitalier, O. Louisnard, R. David, Crystallization of potassium sulphate assisted by ultrasound, Chem. Eng. Trans. 1 (2002) 209–214.

[5] U. Tiepel, I. Mikonsaari, J. Ulrich, Ultrasonic crystallization of potassium alum, Chem. Eng. Trans. 1 (2002) 239–243.

[6] L.H. Thompson, L.K. Doraiswamy, The rate enhancing effect of ultrasound by inducing supersaturation in a solid–liquid system, Chem. Eng. Sci. 55 (2000) 3085–3090.

[7] L.L. Faulkner, S.B. Menkes, Ultrasonics, Fundamentals, Technology, Applications, second ed., Marcel Dekker, Inc., New York, USA, 1988.

[8] R.M. Wagterveld, L. Boels, M.J. Mayer, G.J. Witkamp, Visualization of acoustic cavitation effects on suspended calcite crystals, Ultrason. Sonochem. 18 (2011) 216–225.

[9] N. Amara, B. Ratsimba, A.M. Wilhelm, H. Delmas, Crystallization of potash alum: effect of power ultrasound, Ultrason. Sonochem. 8 (2001) 265–270.

[10] R. Chow, R. Blindt, R. Chivers, M. Povey, A study on the primary and secondary nucleation of ice by power ultrasound, Ultrasonics 43 (2005) 227–230.

[11] Z. Guo, A.G. Jones, N. Li, The effect of ultrasound on the homogeneous nucleation of $BaSO_4$ during reactive crystallization, Chem. Eng. Sci. 61 (2006) 1617–1626.

[12] V.S. Nalajala, V.S. Moholkar, Investigations in the physical mechanism of sonocrystallization, Ultrason. Sonochem. 18 (2011) 345–355.

[13] N. Lyczko, F. Espitalier, O. Louisnard, J. Schwartzentruber, Effect of ultrasound on the induction time and the metastable zone widths of potassium sulphate, Chem. Eng. J. 86 (2002) 233–241.

[14] S.U. Tanrikulu, I. Eroglu, A.N. Bulutcu, S. Ozkar, Crystallization kinetics of ammonium perchlorate in MSMPR crystallizer, J. Cryst. Growth 208 (2000) 533–540.

[15] J.W. Mullin, Crystallization, fourth ed., Elsevier, Butterworth-Heinemann, 2001.

[16] S.J. Jancic, in: S.J. Jancic, E.J. de Jong (Eds.), Industrial Crystallization, vol. 81, North-Holland, 1982.

[17] C.F. Abegg, J.D. Stevens, M.A. Larson, Crystal size distributions in continuous crystallizers when growth rate is size dependent, A.I.Ch.E. J. 14 (1968) 118–122.

[18] J. Garside, S.J. Jancic, Growth and dissolution of potassium–alum crystals in the subsieve size range, A.I.Ch.E. J. 22 (1976) 887–894.

[19] C.C. Harris, A method for the routine measurement of particle shape factors in the sieve range, Nature 187 (1960) 401–403.

[20] A. Matynia, K. Piotrowski, J. Koralewska, Barium sulfate crystallization kinetics in the process of barium ions precipitation by means of crystalline ammonium sulphate addition, Chem. Eng. Proc. 44 (2005) 485–495.

[21] M.M. Mitrovic, A.A. Zekic, Z.Z. Ilic, Connection between the growth rate distribution and the size dependent crystal growth, Chem. Phys. Lett. 361 (2002) 312–316.

[22] H. Miki, T. Terashima, Y. Asakuma, K. Maeda, K. Fukui, Inclusion of mother liquor inside KDP crystals in a continuous MSMPR crystallizer, Sep. Purif. Technol. 43 (2005) 71–76.

[23] H. Miki, R. Fukunaga, Y. Asakuma, K. Maeda, K. Fukui, Distribution of dye into KDP crystals in a continuous MSMPR crystallizer, Sep. Purif. Technol. 43 (2005) 77–83.